RESEARCH ARTICLE

Effect of perchlorate on biocementation capable bacteria and Martian bricks

Swati Dubey[1,2], Shubhanshu Shukla[3,4], Nitin Gupta[5], Rashmi Dixit[3], Punyasloke Bhadury[6], Aloke Kumar[3]*

1 Centre for Earth Sciences, Indian Institute of Science, Bangalore, Karnataka, India, **2** Department of Microbiology and Cell Science, University of Florida, Gainesville, Florida, United States of America, **3** Department of Mechanical Engineering, Indian Institute of Science, Bangalore, Karnataka, India, **4** Indian Space Research Organisation, Bangalore, Karnataka, India, **5** Universite Paris-Saclay, CEA, CNRS, SPEC, Gif-sur-Yvette, France, **6** Integrative Taxonomy and Microbial Ecology Research Group, Department of Biological Sciences, Indian Institute of Science Education and Research, Mohanpur, West Bengal, India

* alokekumar@iisc.ac.in

OPEN ACCESS

Citation: Dubey S, Shukla S, Gupta N, Dixit R, Bhadury P, Kumar A (2026) Effect of perchlorate on biocementation capable bacteria and Martian bricks. PLoS One 21(1): e0340252. https://doi.org/10.1371/journal.pone.0340252

Editor: Rajeev Singh, Satyawati College, University of Delhi, INDIA

Received: May 22, 2025

Accepted: December 18, 2025

Published: January 29, 2026

Data availability statement: All data are provided as plots/figures in the main manuscript and/or supplementary document.

Funding: The author(s) received no specific funding for this work.

Abstract

With the recent discovery of perchlorate (0.5–1%) in Martian regolith, more experiments related to the impact of perchlorate on microbial life are crucial to understanding the possibility of earth life forms that could sustain on the Martian terrain. While we are familiar with the idea of bioconsolidated Martian bricks made via Microbially Induced Calcite Precipitation (MICP), studies on the effect of perchlorate on Martian bricks & biocementation capable microbes have been obscure. In this work, we investigated the effect of perchlorate ($MgClO_4^-$ salt) on a lab-isolated biocementation capable bacteria & Martian bricks bioconsolidated by the same, with 1% perchlorate in Mars Global Simulant-1 (MGS-1). The screening of biocementation-capable bacteria involved phenol red assay for urease activity followed by Scanning Electron Microscopy (SEM) and X-ray diffraction (XRD) study of the precipitate formed through MICP via ureolytic pathway. The biocementation capable bacterium SI_IISc_isolate was found to be phylogenetically closest to *Sporosarcina pasteurii* strain S2135 with a draft genome size of 3.69 Mb. To understand the effect of perchlorate on SI_IISc_isolate, we majorly relied on Gram-staining & SEM. The negative effect of perchlorate stress on the isolate was evident by its decreased growth in the presence of varying concentrations of perchlorate through plate assays, growth curve studies in broth & live-dead staining. Gram-staining study and SEM both revealed that perchlorate induces the release of extracellular matrix (ECM) and promotes clustering of cells by the bacteria, which we termed as 'multicellularity-like behavior.' Further, we constructed Martian bricks with Martian Global Simulant (MGS-1) along with 1% perchlorate, utilizing the microbially induced calcite precipitation ability of the *Sporosarcina* sp. strain SI_IISc_isolate via ureolysis, following an established protocol at our lab. The bioconsolidation experiments showed that in the presence of a natural adhesive

Competing interests: The authors have declared that no competing interests exist.

– guar gum, perchlorate tends to significantly improve the compressive strength of Martian bricks. However, the end result eventually relies on the overall effect of various additives in the regolith.

I. Introduction

Ancient Mars has had a history of water [1–3] and the present Mars has an uncanny resemblance to the early atmosphere of Earth [4]; the red planet is an interesting study into planetary evolution as well as into the origin and evolution of life [5–7]. The red planet has also been identified as a potential candidate for the establishment of a human colony; our intended progression from manned missions into space (Low Earth Orbits) to Mars Missions by 2030, demands extensive research on Mars habitation with a special focus on sustainable and cost-effective methods. In-Situ Resource Utilization (ISRU) is an idea that encourages the utilization of locally available resources for space exploration [8]. An abundant resource on Mars is its regolith [9,10]. The Martian regolith is mostly composed of pyroxenes, olivines, plagioclase, and abundance of iron oxides [11,12]. Along with these minerals, the perchlorates were detected in 2008 by the Phoenix lander [13,14] – a discovery that was confirmed by the instruments on board the Curiosity rover [15,16]. Fig 1 represents the Martian landscape where the landing sites of the rovers and perchlorate detection are delineated.

Research that needs to employ Martian regolith typically employs 'simulants', which simulate closely the content of actual Martian regolith. Earth-based experiments using Martian regolith simulant are an important step towards understanding how Earth-based life can thrive on Mars. For example, the BIOMEX experiment used Martian regolith simulant (MRS) as a substrate to test the viability and growth of *Deinococcus radiodurans* and other microbes on the International Space Station (ISS) [17]. Harris et al. demonstrated soil fertility by studying *Sinorhizobium meliloti*-legume interactions in JSC Mars 1 simulant [18]. However, Earth-based simulants like MGS-1, do not have perchlorate that is present in the actual Martian environment. There are a limited number of studies exploring microbially induced calcite precipitation (MICP) in Martian regolith simulants. For instance, a study demonstrated biocementation using the microalga *Thraustochytrium striatum* for bio-grouting [19]. This study was later extended to optimize the compressive strength of bio-cemented soil columns [20]. Martian bricks have been constructed with Mars Global Simulant-1 (MGS-1) by using a biocementation-capable bacteria *Sporosarcina pasteurii* [21,22], through the mechanism of MICP via ureolysis [23]. However, all these studies share a common limitation: they were conducted without accounting for the presence of perchlorates in the Martian regolith.

Despite the fact that perchlorates are a minority constituent of Martian regolith they are relevant because they have been closely associated with the habitability of the planet. Being a strong oxidant, they can readily degrade organic matter and hence have been claimed to interfere with the detection of biosignatures in the regolith. Since the hydrated perchlorates are seen as sinks for H_2O and have also

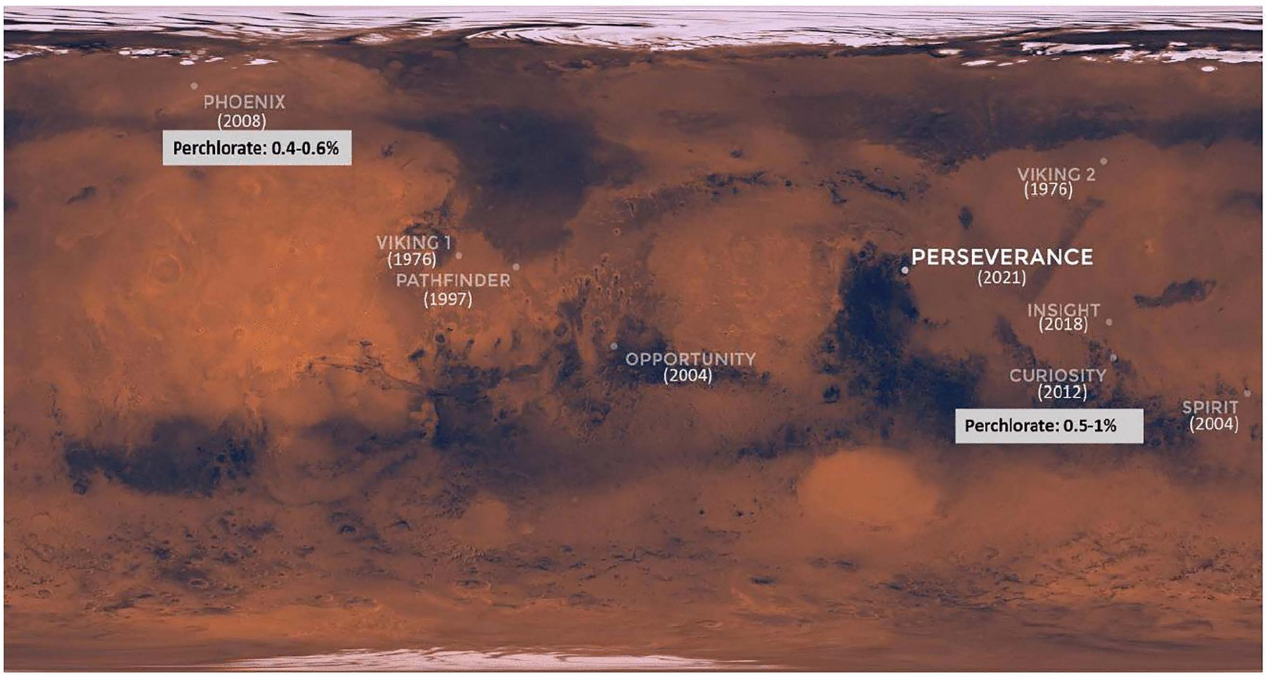

Fig 1. Map showing the landing sites for landers sent by NASA for Mars exploration. The respective landing years are mentioned in brackets. The Mars visit which found perchlorate on the Martian surface is highlighted. Mars map adapted from NASA-JPL/Caltech.

https://doi.org/10.1371/journal.pone.0340252.g001

been shown to inhibit the salt and ice crystallization [24–28], their study in context to regolith and microbial life could yield interesting insights. On Earth, perchlorates are identified as an environmental pollutant, potentially toxic to living cells by causing severe oxidative stress [29–31]. However, certain perchlorate metabolizing bacteria belonging to genera such as *Sedimenticola*, *Marinobacter*, *Azoarcus*, *Dinitromonas,* and *Marinobacter* [32] and perchlorate tolerant bacteria such as *Haloterrigena* sp. strain SGH1 [33], *Halomonas salifodinae* [34,35] are known to us. Most of these microbes are extremophiles- a group that has been most frequently associated with the study of extraterrestrial possibility of life.

Biocementation-capable microbes as our tools of a sustainable Mars habitation through their ability to consolidate the Martian regolith along with their potential to withstand several harsh conditions [36–41], are good candidates for examining the regolith-microbe interaction and are rarely studied with this perspective [42–44].

In our work, we investigated the impact of perchlorate on *Sporosarcina spp*. strain SI_IISc_isolate (hereafter interchangeably called SI) isolated by us. The strain's biocementation capability is identified through biochemical assays, scanning electron microscopy, and X-ray diffraction (XRD) study. 16S rRNA sequencing and whole genome sequencing were done for phylogenetic identification and to identify the metabolic potential of the bacteria. The Minimum Inhibitory Concentration (MIC) of perchlorate for the SI was identified through plate assays and growth curve study, after which the impact of 0.5%, 1%, and 2% perchlorate on the bacteria was studied through optical microscopy after gram-staining and through scanning electron microscopy (SEM). Furthermore, the biocementation ability of SI was explored through the construction of Martian bricks by a previously established protocol using MGS-1 simulant with the addition of 1% perchlorate.

II. Materials and methods

Screening of MICP-capable bacteria

The soil sample was collected from a site in Bangalore, India during March 2021.

The collected soil sample was immediately incubated at 32^0C in Synthetic Media + 2% Urea solution for 24 hrs and microbial isolation was done according to the serial dilution method and subsequently, colonies of distinct different morphologies were selected for further screening. The isolates were subjected to biochemical tests including for carbohydrate utilization using Bacillus Identification Kit (HiMedia, India),(S1 Table and S1 Fig). Gram Staining was done to study the cellular morphology.

Screening for Urease activity

A qualitative phenol red assay was used to determine the ureolytic activity of the isolated strains. Synthetic Media+ 2% Urea (hereby called SMU) along with 0.001% phenol red dye (pH indicator) was used for the assay. Spot inoculation of different colonies was done on the plates followed by incubation for 18–24 hrs at 32^0C. Based on positive results for phenol red assays, bacterial strains were subsequently selected to test for their microbially induced calcite precipitation or MICP ability through the formation of $CaCO_3$ precipitates, via ureolysis.

Microbially Induced Calcite Precipitation (MICP)

For screening the bacterial isolates for their ability to form $CaCO_3$ precipitates in-vitro, 25mM of Calcium Chloride (diluted from 1M of $CaCl_2$ stock solution) was added to synthetic media with 2% urea (SMU) broth. This media was inoculated with the selected bacterial strains in triplicates and left for incubation at 32^0C for 5 days on a shaker incubator (BioBee, India), at a rotating speed of 130 rpm, along with control tubes with no bacterial inoculation.

Scanning Electron Microscopy of the precipitate

Based on the MICP screening, an isolate -referred to as SI_IISc_isolate or SI, was selected. The total precipitate formed by this bacteria was subjected to scanning electron microscopy (SEM) to study the morphology of the precipitate formed in the presence of calcium and urea, by the ureolytic activity of the bacteria, The total precipitate including the cell biomass was therefore fixed with 2.5%glutaraldehyde: 2%formaldehyde PBS buffer (pH 7.4) in the ratio of 1:1:4 for at least 30 min, followed by centrifugation at 5˚C and 5000 rpm for 5 minutes followed by application of standard steps of SEM. Before SEM imaging, dried samples were coated with gold in a sputter coater. Samples were observed under a SEM microscope (Carl Zeiss AG—ULTRA 55, Germany).

X-Ray Diffraction study of the precipitate

To identify the mineral phase of the precipitate formed by SI, an XRD study was done. The precipitate was pelleted down by centrifugation (5000 rpm, 10 min) and then air dried, followed by grinding by mortar and pestle for homogeneity. This precipitate was further analyzed for Powder-XRD study through an X-Ray Diffractometer (PANalytical Philips diffractometer) using CuKα Rays (λ = 1.54056 A), diffraction angle 2θ ranging from 5^0 to 90^0. The raw data was analyzed through X'Pert Highscore Plus Pattern Analysis Software using ICSD (Inorganic Crystal Structure Database) sub-files.

Genomic DNA extraction of SI_IISc_isolate

Bacterial cells were scraped out from the agar plates and suspended in 1 ml of 1X TE (Tris-EDTA, Tris-Cl 10 mM pH 8.0, EDTA 1 mM) before undertaking extraction of genomic DNA. Finally, the pellet was air-dried and dissolved in 1X-TE buffer.

PCR amplification, sequencing of 16S rRNA fragment, and molecular phylogeny

For PCR amplification of the 16S rRNA of SI, two primers 203F and 1492R were used [45]. The PCR reactions were set following the protocol as described earlier. The PCR amplicon was purified and subjected to Sanger sequencing in the ABI 3130xl platform. Based on the blastn result, the top 10 sequences showing hit with the sequence data of SI_IISc isolate

were considered. The sequences were aligned using BioEdit and subsequently, the alignment was subject to ModelTest in MEGA 11. Based on the output of ModelTest, the Maximum Likelihood (ML) tree was constructed with a bootstrap support of 1000. The sequence of the SI_IISc isolate has been submitted to GenBank and the accession number is PP919058.

Whole genome sequencing of SI_IISc isolate

High-quality genomic DNA from SI was extracted using a modified protocol. The whole genome was sequenced on a MinION platform using Oxford Nanopore Technologies (ONT) Sequencing chemistry. The genome library was prepared using a ligation sequencing kit (SQK-LSK109, ONT, UK). The library was purified using magnetic beads (Sergei Lab Supplies LLC, USA) and sequenced on an R9.4.1 Flowcell. The *de novo* genome assembly was filtered for long reads using flye (v2.9.3) [46]. The quality of the assembled genome was evaluated using QUAST (v5.2.0) and annotated using Prokka (v1.14.6) [47]. The genome map was created using Proksee [48].

Effect of perchlorate on SI_IISc_isolate

To understand the effect of perchlorate on the growth of the *Sporosarcina sp*. strain SI_IISc_isolate including inhibition, the minimum inhibitory concentration (MIC) of perchlorate was determined using plate assay and broth tests (S1 File). In both broth and solid media, perchlorate (as magnesium perchlorate) was introduced in the form of a solution in the Synthetic Media with 2% Urea or SMU, as described earlier. To study the effect of perchlorate on SI_IISc isolate at cellular & sub-cellular levels, Gram-staining and SEM were performed in the presence of 0.5%, 1%, and 2% of perchlorate in SMU & Nutrient Broth (HiMedia, India) +2% Urea (NBU) broth media respectively. For gram-stained bacterial cells, imaging was undertaken at 100x magnification under a bright field microscope. (Leica DMi8, USA). Similarly, SEM images of the bacterial cells were undertaken, following the protocol as described earlier. Moreover, to understand the effect of perchlorate on the viability of SI, live/dead staining was performed.

MICP consolidated Martian bricks with perchlorate

The Martian bricks were constructed utilizing the biocementation ability of the *Sporosarcina sp*. strain SI_IISc_isolate using MGS-1 as Martian regolith simulant along with 1% perchlorate by the protocol previously established at our lab [49]. To understand the role of different components of the slurry mixture used for our brick consolidation experiment, various controls were used (discussed later in the results section). The cubical brick samples obtained from this method were uniformly ground and polished using a portable grinder (Bosch GWS 600) to ensure consistent compression behaviour. The final specimens were in the form of cubes with dimensions of 19 ± 1 mm. Finally, the compression strengths of the bricks were evaluated using a Universal Testing Machine (Instron-5697) equipped with a 5 kN capacity load cell and operated at a 0.5 mm/min loading rate.

III. Results and discussion

A. Isolation of MICP-capable bacteria

Microbially induced calcite precipitation. Only one isolate named SI_IISc_isolate gave positive results for urease activity through phenol red assay. The isolate formed amorphous precipitates in the presence of 25mM $CaCl_2$ in Synthetic Media+2% Urea (SMU), after 5 days of incubation (Fig 2). Similar qualitative analysis of ureolytic activity (phenol red plate assay) was performed with different concentrations of perchlorate to understand the impact of perchlorate on the ureolytic activity of bacteria (S2 Fig). SI formed a precipitate in the presence of 25mM $CaCl_2$ in SMU broth after 5 days of incubation at 32° C. The total precipitate hence formed was pelleted down after centrifugation and studied through SEM and X-Ray Diffraction to validate the MICP ability of SI bacteria.

The precipitate formed due to ureolytic activity by SI when observed through SEM showed floret-like precipitates along with rhombohedral nanocrystalline structures which is a characteristic morphology for calcite precipitates. The bacterial cells were also seen wrapped up to the floret-like precipitates (Fig 3a). Analysis of the XRD pattern of the precipitate revealed the presence of calcite peaks along with a few peaks of vaterite and aragonite, as analyzed through X'pert High-Score Plus Pattern Software. Identification of mineral precipitates was done through thoroughly indexed peaks obtained at different 2θ & hkl values along with d-spacing, studied in reference to the available database from the ICSD sub-files. Fig 3b is the graph for the relative intensity at different diffraction angles (2θ), which shows calcite peaks, as identified through thoroughly indexed peaks, for which the intensity values, diffraction angles along with the relevant reference IDs are given in the supporting information. (S2 Table).

Molecular identification and phylogeny of SI_IISc isolate

A gram-positive, facultatively anaerobic bacterial isolate SI_IISc_isolate (inset of Fig 4) gave positive results for phenol red assay and was able to cause calcium carbonate precipitation in-vitro, through its ureolytic activity. The summary of

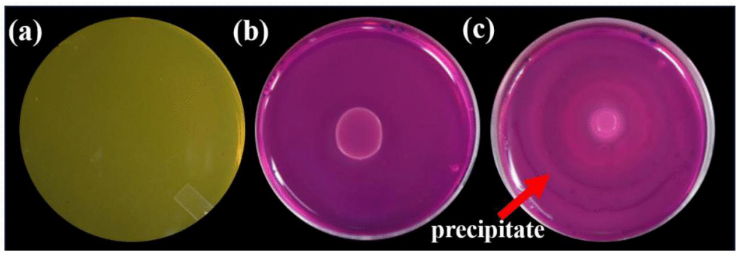

Fig 2. Phenol Red plate Assay for SI_IISc_isolate (also called SI) to test for ureolysis activity. (a) Control_ No bacteria on SMU + 0.001% Phenol Red Dye. **(b)** SI spot inoculated on SMU + Dye. The colour change from yellow to pink represents the pH change of the media from ~5.5 to.8 and above. **(c)** SI spot inoculated on SMU + Dye + 25mM CaCl2. The white lines on the plate represent calcite precipitate. Note: Plate dimensions- 90x14mm.

https://doi.org/10.1371/journal.pone.0340252.g002

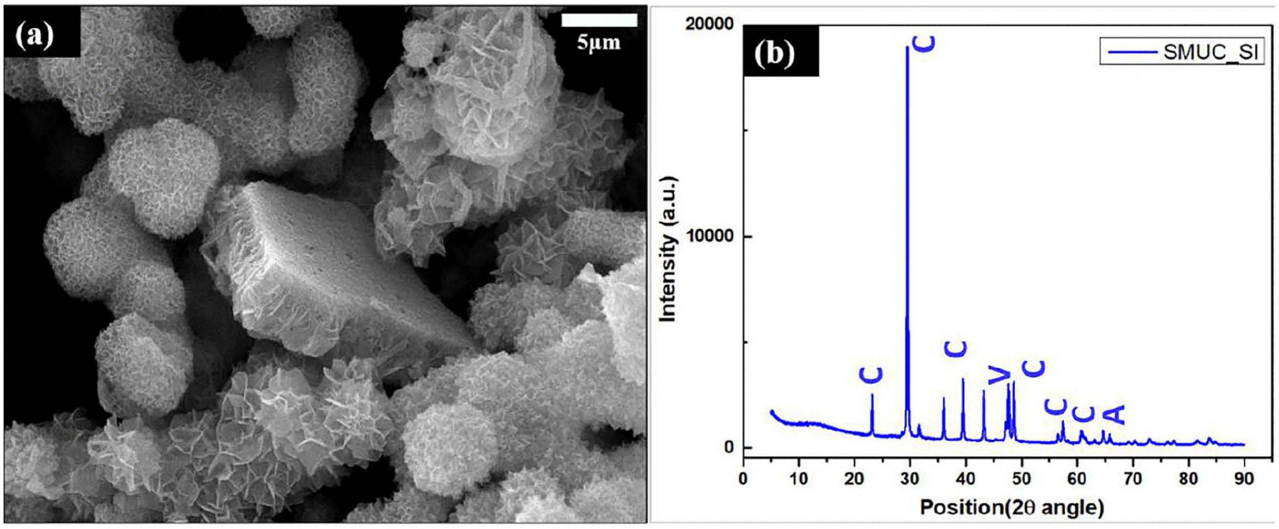

Fig 3. (a) Scanning Electron Microscopy images of the calcite precipitate made by the MICP-capable bacteria SI via its ureolytic activity. (b) X-Ray Diffraction (XRD) results for the precipitate. C represents Calcite, V represents Vaterite, A for aragonite, and peaks as identified through the ICSD database sub-file.

https://doi.org/10.1371/journal.pone.0340252.g003

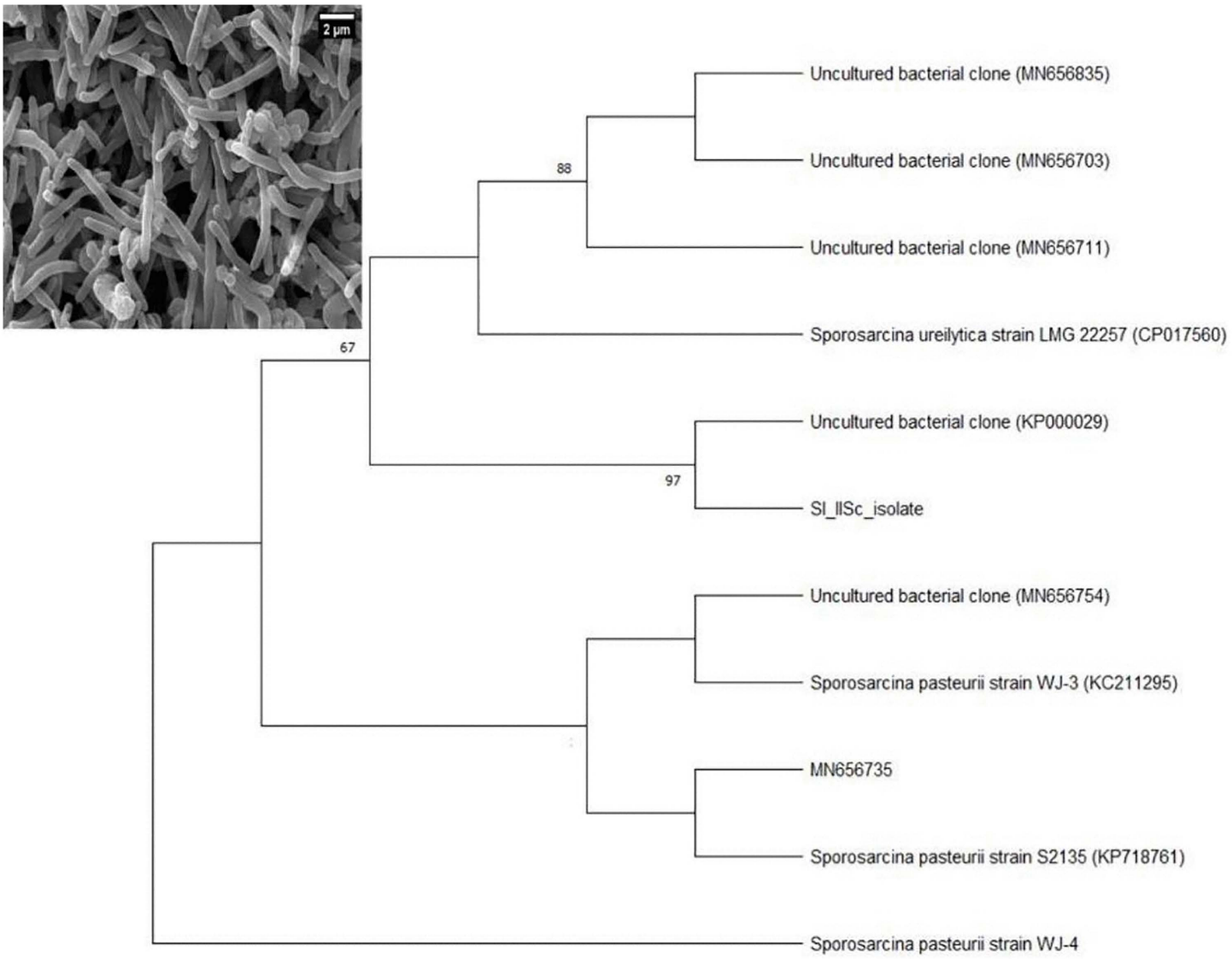

Fig 4. Maximum Likelihood tree of 16S rRNA showing the relationship of SI_IISc isolate with closely related taxa, values in node indicate bootstrap support. Inset is a SEM image of the SI_IISc isolate.

https://doi.org/10.1371/journal.pone.0340252.g004

biochemical test results along with the motility test for the isolate has been given in S1 Table and S1 Fig respectively. Based on blastn analysis, the 16S rRNA sequence of SI_IISc isolate showed 99% identity with *Sporosarcina pasteurii* strain S2135 (Accession Number: 718761), a bacterium that was isolated from the soil environment in China as well as with *Sporosarcina pasteurii* strain WJ-4 (Accession number KC211296), a bacterium isolated from the concrete environment in Korea. Based on ML phylogeny, SI_IISc_isolate clustered with the *Sporosarcina* clade with strong bootstrap support but also indicated that the isolate from this present study could be potentially novel (Fig 4).

The sequenced genome size of *Sporosarcina* sp. strain SI_IISc_isolate is approximately 3.69 Mb in size. The draft genome comprises of 27 ribosomal RNAs, 81 transfer RNAs, 1 transfer messenger RNA (tmRNA), and 4,678 coding sequences (CDS). In total 4678 CDS have been identified from the draft genome (Fig 5). The identified genes (4787)

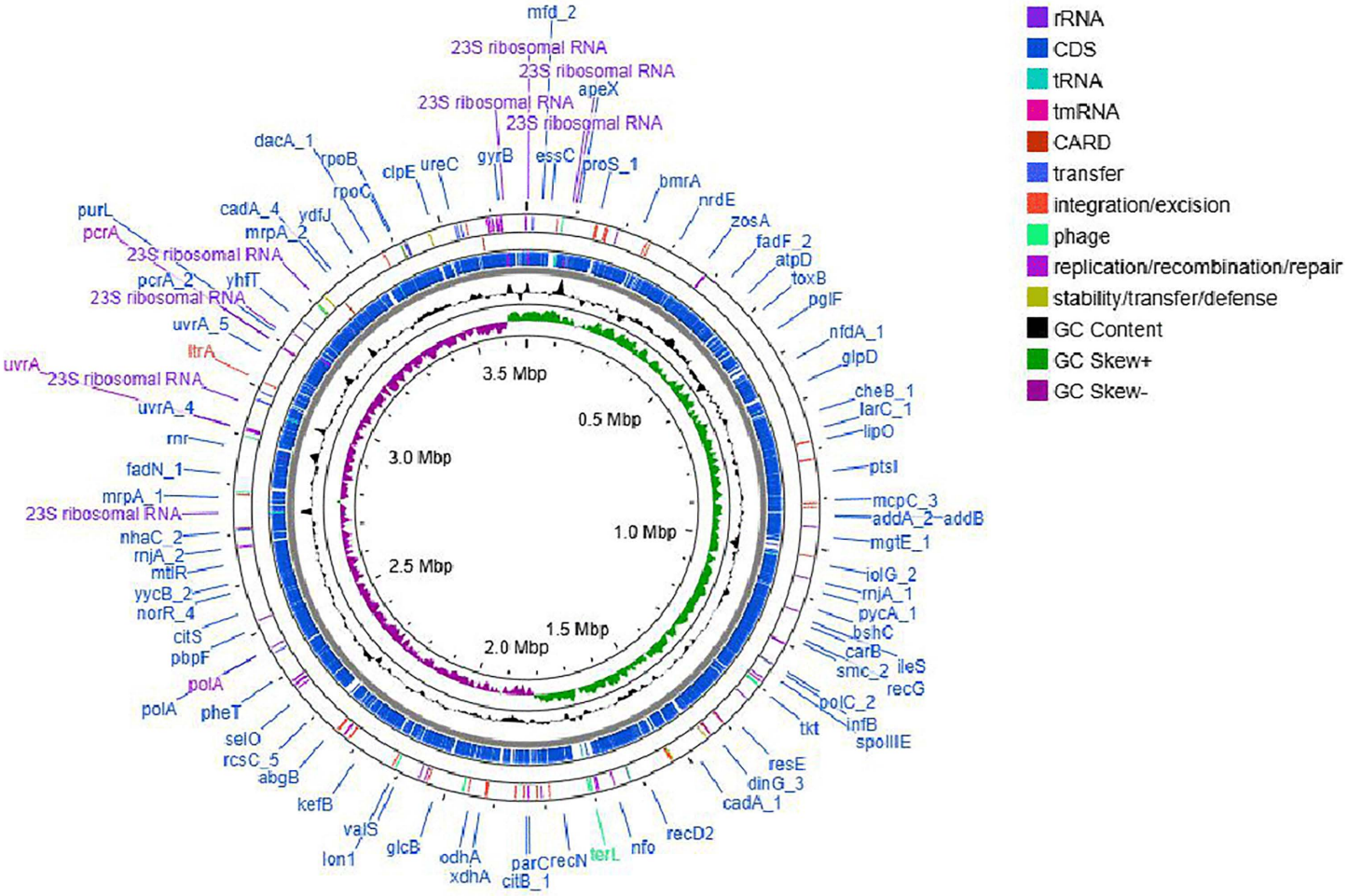

Fig 5. Genome map showing a circular map of the genome (representation only), identified genes, GC Content, and GC Skew of SI_IISc isolate.

https://doi.org/10.1371/journal.pone.0340252.g005

code for many metabolic pathways including for nitrate reductase as well as genes with subunits that code for perchlorate reductase (pcrAB) that play an important role in the utilization of perchlorate. The UreC gene attributing to ureolytic activity within the bacterium has been also identified from the draft genome. The draft genome is available in NCBI database under the BioProject ID: PRJNA1221533 and the BioSample number: SAMN46743258.

B. Effect of perchlorate on SI_IISc_isolate

To know the effect of perchlorate on the growth and viability of the *Sporosarcina sp*. strain SI_IISc_isolate, we performed a growth curve in different concentrations of perchlorate, and the Minimum Inhibitory Concentration (MIC) of perchlorate on this strain was determined to be 3%, through plate and broth assays exhibiting tolerance up to 2% of perchlorate salt. The growth curve experiments showed a gradual decrease in growth of this strain with increasing concentration of perchlorate (S3 and S4 Figs). The negative impact of perchlorate on this strain was also validated through live-dead staining, performed in NBU media in 0.5%, 1%, and 2% concentrations of perchlorate salt along with a control (no perchlorate) set. After 8 hours of incubation, a gradual increase in the number of dead cells was observed with increasing concentrations of

perchlorate salt and the bacterial cell size also diminished under perchlorate's presence (as compared to the control), (S5 Fig).

Based on these results which confirmed that perchlorate was a stressor for this strain; to further study the impact of perchlorate on the biocementation capable bacteria we performed Gram-staining and SEM studies of this isolate in the presence of 0.5%, 1%, and 2% perchlorate. Since perchlorate found in Martian regolith is known to be in the range of 0.5%−1%, we performed our experiments with 0.5%, and 1% along with 2% perchlorate salt concentration with 2% perchlorate concentration as an outlier.

Gram staining. On gram staining the bacterial cells being exposed to different concentrations of perchlorate, we found certain changes in the morphology of the individual cells along with changes in their cells-distribution pattern. Fig 6a–6d shows gram-stained images with their corresponding magnified versions in the insets attached below. Since SI being phylogenetically assigned to *Sporosarcina sp*., is a gram-positive bacterium; the bacterial cells were stained purple, elongated rod-shaped cells as shown in Fig 6a.

On multiple repetitions of the gram-staining experiment, we found that the *Sporosarcina sp*. strain SI_IISc_isolate cells exposed to perchlorate tend to adapt a smaller size & less elongated shape than the control set. A more pronounced change was in the distribution pattern of the cells in response to perchlorate. It was noted that on increasing the concentration of perchlorate, the tendency of bacterial cells to form clusters gradually increased. For example, the bacterial cells exposed to 0.5% perchlorate, showed early signs of clustering by forming small undefined clusters in Fig 6b.as compared to the control in Fig 6a., the cells with 1% perchlorate exposure in Fig 6c., formed very small groups of cells in a better-defined cluster, while the cells in Fig 6d. with 2% perchlorate exposure showed very well-defined clusters formed more repetitively than the other two sets. However, it would be early to comment on whether there was a particular pattern in the clustering which led us to believe that perchlorate's presence encouraged multicellularity- like behaviour in the bacteria. We also noticed that the perchlorate-exposed cells released extracellular matrix (ECM) seen as purple patches or blots on the slide and this response was observed in cells exposed to all three concentrations (0.5%, 1%, 2%) of

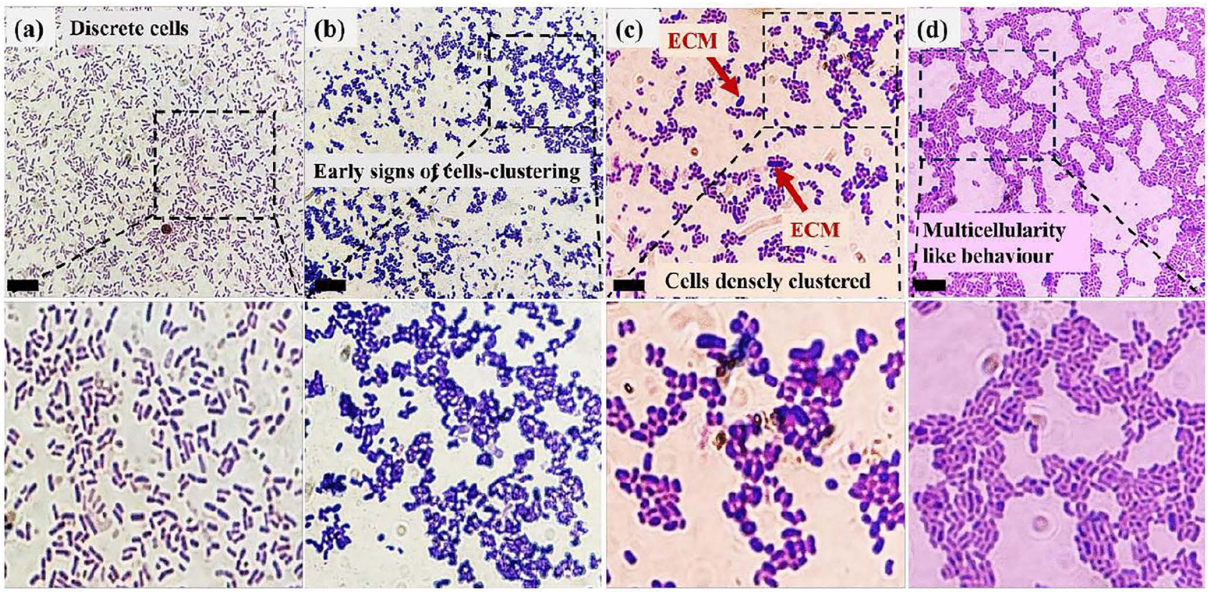

Fig 6. Gram-staining results showing the difference in cell morphology and behaviour of the Sporosarcina sp. strain SI_IISc _isolate(or SI). **(a)** SI Control **(b)** SI + 0.5%Perchlorate **(c)** SI + 1%Perchlorate **(d)** SI + 2%Perchlorate. The lower panel represents magnified portions of corresponding images in the top panel. The scale bar represents 10μm.

https://doi.org/10.1371/journal.pone.0340252.g006

perchlorate, more clearly seen in Fig 6c (indicated by red arrows). This observation was consistent with multiple repeats of the experiment which strongly indicates that perchlorate induced ECM release in cells.

Scanning electron microscopy. For SEM analysis, *Sporosarcina sp*. strain SI_IISc_isolate cells were exposed to 0.5%, 1%, and 2% perchlorate ($MgClO_4^-$ introduced as salt solution) in SMU broth followed by 5 days of incubation after which the cells were centrifuged to obtain a pellet, fixed for SEM study (Fig 7). Fig 7a to 7c, 7d to 7f and 7g to 7i shows SEM images of the total pellet obtained after exposure of this strain to 0.5%, 1%, and 2% perchlorate respectively.

It was observed during and after the incubation period that this strain induced the formation of an inorganic precipitate in the presence of perchlorate which dominated the total pellet. These precipitates can be abundantly seen in the SEM images indicated by blue arrows (morphology most clearly evident in Fig 7g). The chemical nature of this inorganic precipitate could not be identified through XRD due to the pellet's hygroscopic nature and impurity with high organic mass. However, a significant release of extracellular matrix (ECM) also referred to as extrapolymeric substances or EPS in the SEM images can be seen as organic mass more evident in Fig 7a and 7d, indicated by red arrows. No ECM was observed in SEM images of the control – that is bacteria without perchlorate exposure (inset image in Fig 4). The release of ECM was an observation consistent with the gram-staining study and therefore it further validates that perchlorate encouraged the

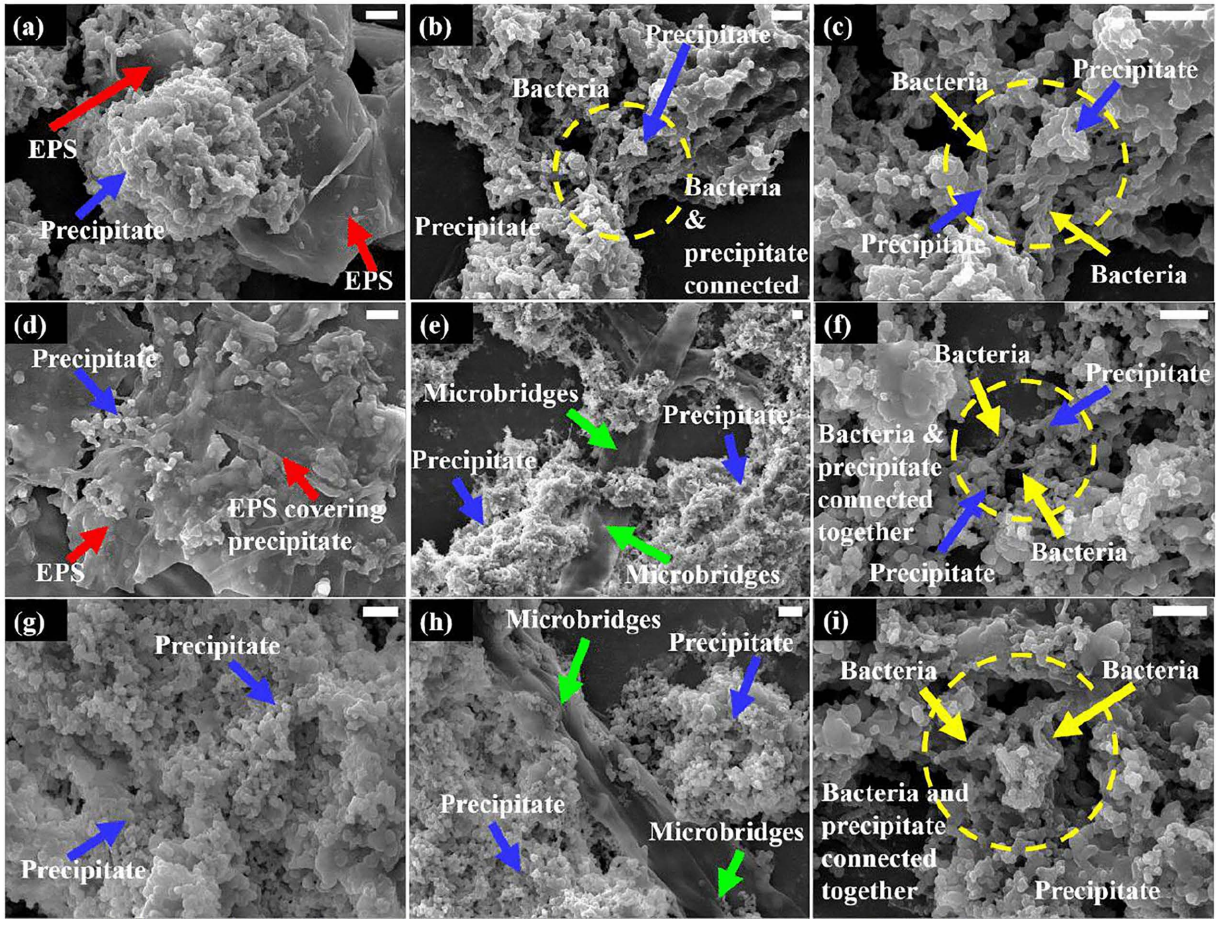

Fig 7. Scanning Electron Microscopy: Images of the total precipitate formed from bacterial exposure to different concentrations of perchlorate (as $(MgClO_4)_2$). (a) to **(c)** SEM images for total precipitate with SI + 0.5%Perchlorate (d) to (f) with SI + 1%Perchlorate & (g) to (i) for SI + 2%Perchlorate. The scale bar represents 5 μm.

https://doi.org/10.1371/journal.pone.0340252.g007

ECM release by this strain. Of special interest were the microbridges – a term we refer to the ECM material acting as a conduit between the salt precipitates and the bacteria (Fig 7e and 7h) indicated by green arrows. The interaction of the inorganic precipitate and bacteria (indicated by yellow arrows) can be easily seen in images 7b, c, f and i, indicated by yellow dotted circles. To ensure the dependability of the images, for each experimental set we showed a panel of three images with variable degrees of magnification such that the bacteria, precipitate and ECM can be observed in a single field of view. For a closer look on interaction of bacteria, precipitates and ECM, please refer to the magnified versions of Fig 7c, 7i, 7f as available in the supplementary information file (S6 and S7 Figs).With increasing concentration of perchlorate, the occurrence of bacterial cells decreased along with significant reduction in ECM release, which could be attributed to the negative impact of perchlorate on the viability of bacterial cells.

C. MICP-consolidated 'Martian bricks' with perchlorate

Compressive strength evaluation. For bioconsolidation of bricks, a blend of the *Sporosarcina sp*. strain SI_IISc culture along with Martian regolith was combined with SMU media in a slurry form and allowed to incubate within the mold cavities for approximately 5 days. Various control experiments were set up simultaneously such as the slurry without perchlorate, guar gum, and nickel chloride respectively, and in different combinations in order to understand the effect of perchlorate on bioconsolidation. The general workflow of the bricks-casting method can be understood by the schematics given below (Fig 8). Following the incubation period, the resulting cubical samples were extracted, dried, and subjected to quasi-static compression tests.

The results of compressive strength measurements derived from different slurries with various media combinations are given in Fig 9. The Martian bricks made with MGS-1 consolidated with deionized (DI) water yielded a very low compressive strength of 0.17MPa and crumbled under self-weight. The bioconsolidation with the culture resulted in a strength comparable to the corresponding abiotic control and the slurry mixture including bacteria along with 1% perchlorate (denoted by SI + P) also yielded similar results with bricks' compressive strength being 0.064 MPa. These results can be attributed to the poly-extreme conditions in the Martian regolith, especially in the presence of perchlorate. However, using 1% guar gum which is a natural adhesive [50], increased the compressive strength of bricks

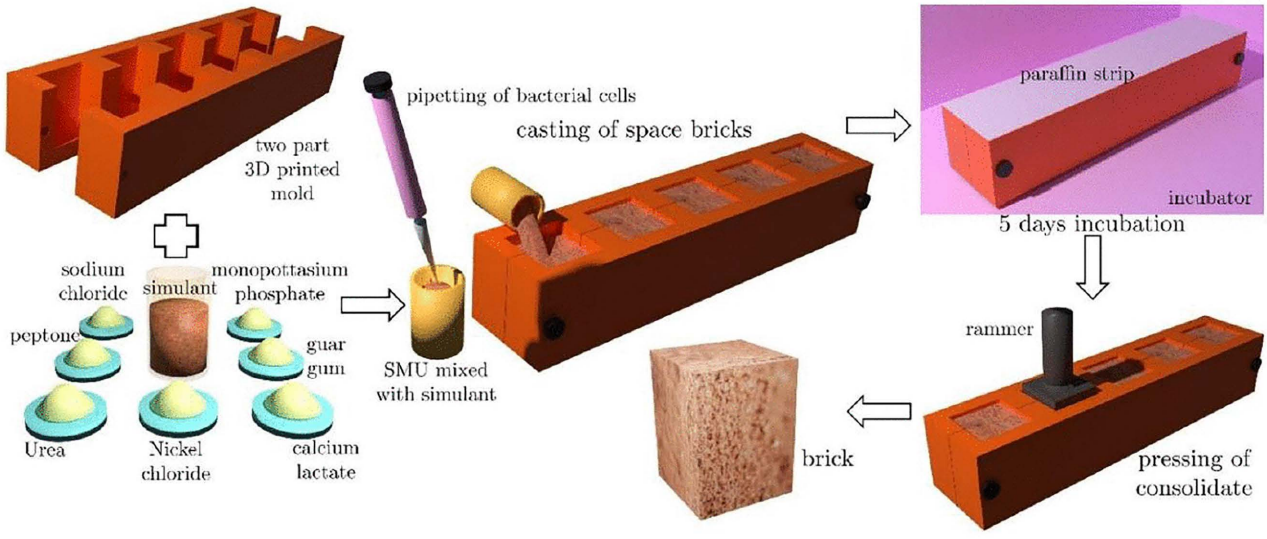

Fig 8. Schematic depicting the brick casting procedure alongside the consolidation process facilitated by MICP in simulated regolith.

https://doi.org/10.1371/journal.pone.0340252.g008

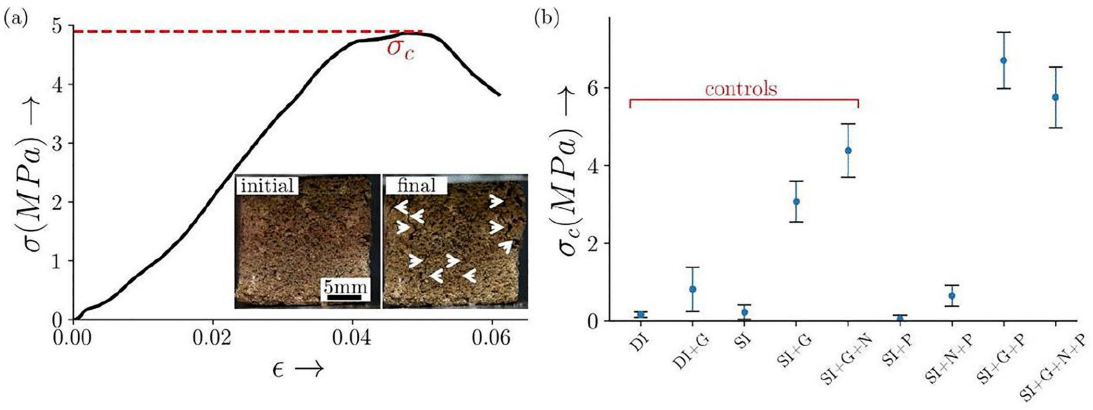

Fig 9. Panel (a) illustrates the stress-strain behaviour of the bio-consolidated specimen subjected to compressive loading. The peak stress observed was designated as the compressive strength σ_c of the consolidated brick. The inset provides a visual representation of the Martian brick specimen 's (made with Martian regolith+ SI + G + N + P) condition during loading, displaying the initial state of the specimen on the left and its final state on the right, with arrows indicating the locations of cracks. Panel (b) presents the compressive strength σ_c, averaged from a minimum of four specimens across various treatment conditions. Error bars indicate the variability in brick strength. The treatments DI and DI + G were treated as a control to check for the significance of MICP and compared with SI and SI + G, respectively. The treatments examined include SI, SI + G, and SI + G + N, serving as controls to assess the influence of perchlorate on the compressive strength of the bricks, a control to check for the significance of MICP and compared with SI and SI + G, respectively. The treatments examined include SI, SI + G, and SI + G + N, serving as controls(i.e., without perchlorate) to assess the influence of perchlorate on the compressive strength of the bricks, a measure indicative of MICP mediation.

https://doi.org/10.1371/journal.pone.0340252.g009

to 0.82MPa in the abiotic control (denoted by DI + G) and to 3.07MPa in the regolith mixture with bacteria (SI + G). This highlights the crucial role of guar gum in significantly encouraging the consolidation process and also confirms the contribution of this strain towards bioconsolidation aided by guar gum. The nickel combined with this strain and 1% perchlorate (SI + N + P) showed a ten-fold increase in the compressive strength, it being 0.64MPa, as compared to the corresponding control without nickel (SI + P). The compressive strength of bacteria with guar gum and nickel (SI + G + N) was 4.4MPa as compared to the without nickel mixture (SI + G, σ_c being 3.07MPa). These observations validated the role of nickel, a known catalyst for ureolysis [51], towards improved bioconsolidation via ureolysis-induced MICP.

On the other hand, the compressive strength of bacteria with guar gum including 1% perchlorate (SI + G + P) was noted to be 6.71MPa, which was almost twice the compressive strength of the corresponding bricks without perchlorate control (SI + G). The bricks made with the bacteria, perchlorate, guar gum and nickel (SI + G + N + P) also showed higher compressive strength being 5.77MPa as compared to the corresponding without perchlorate set (SI + G + N) with σ_c being 4.4MPa. These results indicate that perchlorate enhanced the biocementation process in the presence of bacteria, where the role of guar gum was critical, acting as an adhesive and possibly a source of nutrition helping bacteria to survive the Martian regolith's high salt conditions. However, comparing the SI + G + N + P sample as compared to the without perchlorate set (SI + G + N) showed a little decrease in the bricks' compressive strength which can be attributed to the high metals/ions stress to the bacteria due to the presence of nickel and perchlorate together, making bacterial survivability a bit challenging.

To conclude, these experiments showed that in the presence of 1% guar gum-an important binding agent; the bacteria showed efficient biocementation via ureolysis-induced MICP, improved further in the presence of 1% perchlorate. The role of nickel in improving biocementation was also identified. Overall, these findings underscore the complexity of MICP-mediated consolidation and the significance of understanding the interplay between various additives for optimizing strength in the Martian regolith-based constructions.

IV. Discussion

The bacterial extracellular matrix with or without biofilm in particular is known to encourage cells migration [52], genetic exchange, capturing of ions, cell signalling. & has been frequently correlated with environmental stress as a means of protecting the cells against antibiotics, heavy metals stress, oxidative stress or to overcome the lack of nutrients etc [53–56].

In an experiment with *Bacillus cereus*, high calcium concentration acted as a stress for the bacteria in response to which, the bacteria released ECM [57]. Since our experiments clearly indicate that perchlorate acts as a stressor for the *Sporosarcina sp*. strain SI_IISc, the release of ECM is likely a coping mechanism that can be validated with further studies. In the same experiment with *B. cereus,* ECM has been seen as a link between biofilm and the mineralization ability of the bacteria. However, in our case, more experiments would be required to examine that. In another study with *S. aureus* biofilms, their ECM material was seen as a means of connecting the microbes together suggesting a communication between the multicellular communities. The ECM and microbridges as seen in our SEM images in Fig 6 had a similar appearance to the fibril-like ECM material of *S. aureus* biofilm as seen in the A-SEM (Atmospheric-SEM) study [58].

Multicellularity in bacteria is now a more frequently recognized behaviour [59,60] associated with cell communication, cell-cell adhesion, biofilm formation etc. [61]. The assembly of discrete cells in a small group is considered to be the early stages of multicellularity leading to well-defined patterned clusters later. The SI_IISc_isolate with increasing concentrations of perchlorate exposure showed a greater tendency to form clusters resembling the early stages of multicellularity, where individual cells assembled into small groups. However, since it remains unclear whether these clusters arise from coordinated interactions or developmental organization typical of true multicellularity, the phenomenon that SI_IISc-isolate cells showed in presence of perchlorate is more accurately described as “multicellularity-like behaviour”-that is, cell aggregation that visually mimics the multicellular organization without confirmed evidence of functional multicellularity. To confirm bacterial aggregation as evidence of multicellularity, further studies at the genetic and gene-expression level are required. In a study, *S. aureus* & *E.coli* exposed to high salinity conditions tended to grow in clusters rather than in planktonic state. A similar behaviour of environmentally induced cell-clustering was shown by *Citrobacter freundii* and *Pseudomonas aeruginosa* [62]. This supports our idea of stress-induced multicellularity-like behaviour in SI_IISc_isolate as a response towards perchlorate.

The sequencing and analysis of the draft genome of SI_IISc isolate revealed the presence of plethora of genes that supports the ability of this microbe to adapt to dynamic environmental gradients including in presence of perchlorate. Within the genome, genes with subunit such as pcrAB have been identified that are known to code for perchlorate reductase and thus may have resulted in the metabolic adaptability in presence of varying concentrations of perchlorate. Besides, sequences with homology to *cld* genes were identified from the genome and thus support the ability of this isolate to metabolize perchlorate. In future, the functional significance of these identified genes could be explored from this isolate to track potential upregulation or downregulation in presence of changing gradients of perchlorate. Besides, a number of flagellar proteins have been identified from the genome linked to the ability of this isolate for motility and thus may adapt to stress and multicellularity. The isolate produced EPS in dynamic environmental gradients and the presence of pathways such as Wzx/Wzy-dependent pathway, ABC transporter-dependent pathway and synthase-dependent pathway identified from the sequenced genome indicate functional adaptive capabilities.

The contribution of guar gum’s organic macromolecules towards augmentation of MICP by *Bacillus velezensis* has been established at our lab previously, where the results strongly indicated that guar gum supplementation encourages ureolysis by possibly aiding microbial survivability[51]. Our present work verifies the significant role of guar gum towards biocementation & hence continues to support the inference. Since perchlorate’s role in MICP-induced bioconsolidation of Martian regolith has been rarely explored, this study is an important insight into the Martian bricks construction via ISRU.

V. Conclusion

This work is a preliminary investigation into the impact of perchlorate on (a) a lab-isolated biocementation capable bacteria phylogenetically assigned to be *Sporosarcina sp.* strain SI_IISc. (b) Martian bricks, made with MGS-1 + 1% perchlorate bioconsolidated via ureolysis-induced MICP by this strain, through an already established protocol at our lab. The results of this study suggest that perchlorate acts as a strong stress stimulus for the SI_IISc_isolate as validated by a growth curve study in broth, plate assays & live-dead staining. Multicellularity-like behaviour shown by the bacteria, observed through gram-staining images and extracellular matrix released by the bacteria observed both in gram staining & SEM images further indicated that perchlorate acted as a potent stressor for the bacteria. In SEM analysis, the extracellular matrix was observed to form microbridges, connecting the bacteria and precipitate suggesting a possible exchange between the bacteria and the precipitate.

On the other hand, the bioconsolidation experiments with Martian bricks confirmed that the biocementation capable bacteria isolated at our lab could consolidate the Martian regolith through its ureolytic activity. However, guar gum was found to be imperative for bioconsolidation, without which we could not obtain bricks of considerable compressive strength. This can be explained by guar gum's nutritive properties for the bacteria and its role as a natural adhesive for the bricks' consolidation. The role of $NiCl_2$ as a catalyst was known through the bricks' compressive strength which was improved as compared to the corresponding sample without nickel. In the presence of guar gum, the brick samples with perchlorate tended to have improved compressive strength as compared to the corresponding control samples without perchlorate. A possible reason for this could be the formation of inorganic precipitates by the bacteria or the ECM material released by them (as observed in SEM images) which are possibly acting as binding agents. However, more studies would be needed to establish the cause. Overall, the role of various additives – guar gum, nickel, and perchlorate towards MICP-induced bioconsolidation was highlighted in the study, which underlined the complex interaction between the bacteria, regolith components, and the additives for an efficient biocementation.

Supporting information

S1 File. Supplementary methods.
(PDF)

S1 Table. Summary of Biochemical tests done for SI_IISc_isolate bacteria.
(DOCX)

S1 Fig. Motility test for the SI_IISc_isolate. The bacteria was introduced through an inoculation needle in Nutrient broth +2%Urea(NBU)agar media in the test tube and incubated for 48hrs at 32^0C. Since the bacterial streak has grown along the line of inoculation only, shows negative result for motility.
(TIF)

S2 Fig. Phenol red plate assay (using SMU + 0.001%Phenol Red pH indicator dye) for the strain with varying concentrations of perchlorate. (a) Control experiment with the strain (b) bacterial spot inoculation on plate with 0% perchlorate (c), (d) and (e) represents inoculation with 1%, 2% and 3% perchlorate respectively. Precipitates can be seen as white region on the plate. Ureolytic activity decreases gradually with increasing perchlorate concentration. Note: Plate dimensions- 90*14 mm.
(TIF)

S2 Table. 2Theta values and d-spacing as matched by ICSD database (reference IDs given) through X-Ray Diffraction study of the precipitate made by SI through its ureolysis activity. The data analysis was done through X'Pert HighScore Plus Pattern Software.
(DOCX)

S3 Fig. Growth curve for SI_IISc_isolate in Synthetic Media + 2% Urea (SMU)broth with different concentrations of perchlorate. A) growth curve for SI-(Control-No Perchlorate), B) SI + 0.5% perchlorate C) SI + 1% perchlorate D) SI + 2%perchlorate E) SI + 3% perchlorate salt. As evident from the graph, growth of SI_IISc bacteria decreases with increasing concentration of perchlorate in the media.
(TIF)

S4 Fig. Minimum Inhibitory Concentration (MIC) of Perchlorate for SI_IISc bacteria. Plate Assay- shows SI_IISc_isolate (or SI) bacteria spot inoculation on Nutrient Agar plates in different concentrations of Perchlorate. (a)SI + NBU (Control), 1(b) SI + 0.5% Perchlorate 1(c) SI + 1%Perchlorate 1(d) SI + 2%Perchlorate & (e) SI + 3%Perchlorate. The decrease in bacterial growth is validated by decrease in diameter of bacterial spot growth, which diminishes to be zero (no growth) in (e). Note: Plate dimensions- 90*14 mm.
(TIF)

S5 Fig. Live/dead staining results after after 8 hours of incubation in Nutrient Broth +2% Urea with different concentration of perchlorate as $MgClO_4$. (a) SI(Control), (b) SI + 0.5% Perchlorate (c) SI + 1% Perchlorate (d) SI + 2% Perchlorate. Live cells appear green while the red fluorescence represent dead cells. With increasing concentration of perchlorate, the count of dead cells increased.
(TIF)

S6 Fig. SEM images for SI with 1% perchlorate at two different magnifications. (a) 4000x and (b) 10,000x respectively.
(TIF)

S7 Fig. SEM images of the bacteria in (a) 0.5% perchlorate (b) 1% perchlorate (c) 2% perchlorate. The zoomed-in versions of (a)-(c) are placed below each image respectively, in which the bacteria and precipitate can be clearly seen interacting together. These figures are derived from figures 7(c), (f) & (i) from the paper, for enhanced magnification. The labelling for bacteria and precipitate is not done in these images to avoid over-crowding and for clarity. Scale bar represents 5μm..
(TIF)

Author contributions

Conceptualization: Aloke Kumar.

Data curation: Swati Dubey, Shubhanshu Shukla, Punyasloke Bhadury.

Formal analysis: Aloke Kumar, Swati Dubey, Shubhanshu Shukla, Punyasloke Bhadury.

Investigation: Swati Dubey, Shubhanshu Shukla, Nitin Gupta, Rashmi Dixit.

Methodology: Aloke Kumar, Swati Dubey, Punyasloke Bhadury.

Project administration: Aloke Kumar.

Writing – original draft: Aloke Kumar, Swati Dubey, Shubhanshu Shukla, Nitin Gupta, Punyasloke Bhadury.

References

1. Joseph RG, Dass RS, Rizzo V, Cantasano N, Bianciardi G. Evidence of life on Mars?. J Astrobiol Space Sci Rev. 2019.
2. Squyres SW. The history of water on Mars!. Annu Rev Earth Planet Sci. 1984.
3. Fisher DA. Mars' water isotope (D/H) history in the strata of the North Polar Cap: inferences about the water cycle. Icarus. 2007;187(2):430–41. https://doi.org/10.1016/j.icarus.2006.10.032
4. Carr CE. Resolving the history of life on earth by seeking life as we know it on Mars. Astrobiology. 2022;22(7):880–8. https://doi.org/10.1089/ast.2021.0043 PMID: 35467949

5. Ansari AH. Detection of organic matter on Mars, results from various Mars missions, challenges, and future strategy: a review. Front Astron Space Sci. 2023;10. https://doi.org/10.3389/fspas.2023.1075052
6. Warren-Rhodes KA, Lee KC, Archer SDJ, Cabrol N, Ng-Boyle L, Wettergreen D, et al. Subsurface microbial habitats in an extreme desert mars-analog environment. Front Microbiol. 2019;10:69. https://doi.org/10.3389/fmicb.2019.00069 PMID: 30873126
7. Fairén AG, Davila AF, Lim D, Bramall N, Bonaccorsi R, Zavaleta J, et al. Astrobiology through the ages of Mars: the study of terrestrial analogues to understand the habitability of Mars. Astrobiology. 2010;10(8):821–43. https://doi.org/10.1089/ast.2009.0440 PMID: 21087162
8. Dikshit R, Gupta N, Kumar A. Microbial endeavours towards extra-terrestrial settlements. J Indian Inst Sci. 2023;103(3):839–55. https://doi.org/10.1007/s41745-023-00383-8
9. Scott AN, Oze C, Tang Y, O'Loughlin A. Development of a Martian regolith simulant for in-situ resource utilization testing. Acta Astronautica. 2017;131:45–9. https://doi.org/10.1016/j.actaastro.2016.11.024
10. Fackrell LE, Schroeder PA, Thompson A, Stockstill-Cahill K, Hibbitts CA. Development of martian regolith and bedrock simulants: potential and limitations of martian regolith as an in-situ resource. Icarus. 2021;354:114055. https://doi.org/10.1016/j.icarus.2020.114055
11. Ehlmann BL, Edwards CS. Mineralogy of the martian surface. Annu Rev Earth Planet Sci. 2014;42(1):291–315. https://doi.org/10.1146/annurev-earth-060313-055024
12. Banin A, Ben-Shlomo T, Margulies L, Blake DF, Mancinelli RL, Gehring AU. The nanophase iron mineral(s) in Mars soil. J Geophys Res. 1993;98(E11):20831–53. https://doi.org/10.1029/93je02500
13. Kounaves SP, Hecht MH, West SJ, Morookian J, Young SMM, Quinn R, et al. The MECA wet chemistry laboratory on the 2007 Phoenix Mars scout lander. J Geophys Res. 2009;114(E3). https://doi.org/10.1029/2008je003084
14. Smith PH, Tamppari L, Arvidson RE, Bass D, Blaney D, Boynton W, et al. Introduction to special section on the Phoenix mission: landing site characterization experiments, mission overviews, and expected science. J Geophys Res. 2008;113(E3). https://doi.org/10.1029/2008je003083
15. Ming DW, Archer PD Jr, Glavin DP, Eigenbrode JL, Franz HB, Sutter B, et al. Volatile and organic compositions of sedimentary rocks in Yellowknife Bay, Gale crater, Mars. Science. 2014;343(6169):1245267. https://doi.org/10.1126/science.1245267 PMID: 24324276
16. Stroble ST, McElhoney KM, Kounaves SP. Comparison of the Phoenix mars lander WCL soil analyses with Antarctic dry valley soils, Mars meteorite EETA79001 sawdust, and a Mars simulant. Icarus. 2013;225(2):933–9. https://doi.org/10.1016/j.icarus.2012.08.040
17. de Vera J-P, Alawi M, Backhaus T, Baqué M, Billi D, Böttger U, et al. Limits of life and the habitability of Mars: The ESA space experiment BIOMEX on the ISS. Astrobiology. 2019;19(2):145–57. https://doi.org/10.1089/ast.2018.1897 PMID: 30742496
18. Harris F, Dobbs J, Atkins D, Ippolito JA, Stewart JE. Soil fertility interactions with Sinorhizobium-legume symbiosis in a simulated Martian regolith; effects on nitrogen content and plant health. PLoS One. 2021;16(9):e0257053. https://doi.org/10.1371/journal.pone.0257053 PMID: 34587163
19. Gleaton J, Lai Z, Xiao R, Chen Q, Zheng Y. Microalga-induced biocementation of Martian regolith simulant: effects of biogrouting methods and calcium sources. 2019;2(3).
20. Gleaton J, Lai Z, Xiao R, Zhang K, Chen Q, Zheng Y. Optimization of mechanical strength of biocemented martian regolith simulant soil columns. 2021.
21. Dikshit R, Gupta N, Dey A, Viswanathan K, Kumar A. Microbial induced calcite precipitation can consolidate martian and lunar regolith simulants. PLoS One. 2022;17(4):e0266415. https://doi.org/10.1371/journal.pone.0266415 PMID: 35421143
22. Kumar A, Dikshit R, Gupta N, Jain A, Dey A, Nandi A, et al. Bacterial growth induced biocementation technology, 'Space-Brick' - a proposal for experiment at microgravity and planetary environments. openRxiv. 2020. https://doi.org/10.1101/2020.01.22.914853
23. Ghosh T, Bhaduri S, Montemagno C, Kumar A. Sporosarcina pasteurii can form nanoscale calcium carbonate crystals on cell surface. PLoS One. 2019;14(1):e0210339. https://doi.org/10.1371/journal.pone.0210339 PMID: 30699142
24. Clark BC, Kounaves SP. Evidence for the distribution of perchlorates on Mars. Inter J Astrobiol. 2015;15(4):311–8. https://doi.org/10.1017/s1473550415000385
25. Martínez-Pabello PU, Walls X. Production of perchlorates and nitrates by electric discharges in dust devils on Mars. In: Revista Mexicana de Astronomia y Astrofisica: Serie de Conferencias, 2023. 77–9. https://doi.org/10.22201/ia.14052059p.2023.55.21
26. Kounaves SP, Carrier BL, O'Neil GD, Stroble ST, Claire MW. Evidence of martian perchlorate, chlorate, and nitrate in Mars meteorite EETA79001: implications for oxidants and organics. Icarus. 2014;229:206–13. https://doi.org/10.1016/j.icarus.2013.11.012
27. Kounaves SP, Chaniotakis NA, Chevrier VF, Carrier BL, Folds KE, Hansen VM, et al. Identification of the perchlorate parent salts at the Phoenix Mars landing site and possible implications. Icarus. 2014;232:226–31. https://doi.org/10.1016/j.icarus.2014.01.016
28. Archer PD Jr, Franz HB, Sutter B, Arevalo RD Jr, Coll P, Eigenbrode JL, et al. Abundances and implications of volatile-bearing species from evolved gas analysis of the Rocknest aeolian deposit, Gale Crater, Mars. JGR Planets. 2014;119(1):237–54. https://doi.org/10.1002/2013je004493
29. Zhao X, Zhou P, Chen X, Li X, Ding L. Perchlorate-induced oxidative stress in isolated liver mitochondria. Ecotoxicology. 2014;23(10):1846–53. https://doi.org/10.1007/s10646-014-1312-9 PMID: 25139032
30. Acevedo-Barrios R, Sabater-Marco C, Olivero-Verbel J. Ecotoxicological assessment of perchlorate using in vitro and in vivo assays. Environ Sci Pollut Res Int. 2018;25(14):13697–708. https://doi.org/10.1007/s11356-018-1565-6 PMID: 29504076
31. Niziński P, Błażewicz A, Kończyk J, Michalski R. Perchlorate – Properties, toxicity and human health effects: An updated review. In:Reviews on Environmental Health. De Gruyter Open Ltd; 2021.199–222.https://doi.org/10.1515/reveh-2020-0006

32. Carlström CI, Lucas LN, Rohde RA, Haratian A, Engelbrektson AL, Coates JD. Characterization of an anaerobic marine microbial community exposed to combined fluxes of perchlorate and salinity. Appl Microbiol Biotechnol. 2016;100(22):9719–32. https://doi.org/10.1007/s00253-016-7780-5 PMID: 27596621

33. Díaz-Rullo J, Rodríguez-Valdecantos G, Torres-Rojas F, Cid L, Vargas IT, González B, et al. Mining for perchlorate resistance genes in microorganisms from sediments of a hypersaline pond in Atacama Desert, Chile. Front Microbiol. 2021;12:723874. https://doi.org/10.3389/fmicb.2021.723874 PMID: 34367123

34. Oren A, Elevi Bardavid R, Mana L. Perchlorate and halophilic prokaryotes: implications for possible halophilic life on Mars. Extremophiles. 2014;18(1):75–80. https://doi.org/10.1007/s00792-013-0594-9 PMID: 24150694

35. Matsubara T, Fujishima K, Saltikov CW, Nakamura S, Rothschild LJ. Earth analogues for past and future life on Mars: isolation of perchlorate resistant halophiles from Big Soda Lake. Inter J Astrobiol. 2016;16(3):218–28. https://doi.org/10.1017/s1473550416000458

36. Miot J, Benzerara K, Morin G, Kappler A, Bernard S, Obst M, et al. Iron biomineralization by anaerobic neutrophilic iron-oxidizing bacteria. Geochimica et Cosmochimica Acta. 2009;73(3):696–711. https://doi.org/10.1016/j.gca.2008.10.033

37. Rawlings DE. Characteristics and adaptability of iron- and sulfur-oxidizing microorganisms used for the recovery of metals from minerals and their concentrates. Microb Cell Fact. 2005;4(1):13. https://doi.org/10.1186/1475-2859-4-13 PMID: 15877814

38. Hallberg KB, González-Toril E, Johnson DB. Acidithiobacillus ferrivorans, sp. nov.; facultatively anaerobic, psychrotolerant iron-, and sulfur-oxidizing acidophiles isolated from metal mine-impacted environments. Extremophiles. 2010;14(1):9–19. https://doi.org/10.1007/s00792-009-0282-y PMID: 19787416

39. Lopez-Adams R, Fairclough SM, Lyon IC, Haigh SJ, Zhang J, Zhao F-J, et al. Elucidating heterogeneous iron biomineralization patterns in a denitrifying As(iii)-oxidizing bacterium: implications for arsenic immobilization. Environ Sci Nano. 2022;9(3):1076–90. https://doi.org/10.1039/d1en00905b PMID: 35663418

40. Heinz J, Waajen AC, Airo A, Alibrandi A, Schirmack J, Schulze-Makuch D. Bacterial growth in chloride and perchlorate brines: halotolerances and salt stress responses of Planococcus halocryophilus. Astrobiology. 2019;19(11):1377–87. https://doi.org/10.1089/ast.2019.2069 PMID: 31386567

41. Mastascusa V, Romano I, Di Donato P, Poli A, Della Corte V, Rotundi A, et al. Extremophiles survival to simulated space conditions: an astrobiology model study. Orig Life Evol Biosph. 2014;44(3):231–7. https://doi.org/10.1007/s11084-014-9397-y PMID: 25573749

42. Acevedo-Barrios R, Tirado-Ballestas I, Bertel-Sevilla A, Cervantes-Ceballos L, Gallego JL, Leal MA, et al. Bioprospecting of extremophilic perchlorate-reducing bacteria: report of promising Bacillus spp. isolated from sediments of the bay of Cartagena, Colombia. Biodegradation. 2024;35(5):601–20. https://doi.org/10.1007/s10532-024-10079-0 PMID: 38625437

43. Schultz J, dos Santos A, Patel N, Rosado AS. Life on the edge: bioprospecting extremophiles for astrobiology. J Indian Inst Sci. 2023;103(3):721–37. https://doi.org/10.1007/s41745-023-00382-9

44. Serrano P, Alawi M, de Vera J-P, Wagner D. Response of methanogenic archaea from siberian permafrost and non-permafrost environments to simulated mars-like desiccation and the presence of perchlorate. Astrobiology. 2019;19(2):197–208. https://doi.org/10.1089/ast.2018.1877 PMID: 30742498

45. Wawrik B, Kerkhof L, Zylstra GJ, Kukor JJ. Identification of unique type II polyketide synthase genes in soil. Appl Environ Microbiol. 2005;71(5):2232–8. https://doi.org/10.1128/AEM.71.5.2232-2238.2005 PMID: 15870305

46. Kolmogorov M, Yuan J, Lin Y, Pevzner PA. Assembly of long, error-prone reads using repeat graphs. Nat Biotechnol. 2019;37(5):540–6. https://doi.org/10.1038/s41587-019-0072-8 PMID: 30936562

47. Seemann T. Prokka: rapid prokaryotic genome annotation. Bioinformatics. 2014;30(14):2068–9. https://doi.org/10.1093/bioinformatics/btu153 PMID: 24642063

48. Grant JR, Enns E, Marinier E, Mandal A, Herman EK, Chen C-Y, et al. Proksee: in-depth characterization and visualization of bacterial genomes. Nucleic Acids Res. 2023;51(W1):W484–92. https://doi.org/10.1093/nar/gkad326 PMID: 37140037

49. Dikshit R, Dey A, Gupta N, Varma SC, Venugopal I, Viswanathan K, et al. Space bricks: from LSS to machinable structures via MICP. Ceramics Inter. 2021;47(10):14892–8. https://doi.org/10.1016/j.ceramint.2020.07.309

50. Dikshit R, Jain A, Dey A, Kumar A. Microbially induced calcite precipitation using Bacillus velezensis with guar gum. PLoS One. 2020;15(8):e0236745. https://doi.org/10.1371/journal.pone.0236745 PMID: 32785276

51. Mazzei L, Cianci M, Benini S, Ciurli S. The structure of the elusive urease–urea complex unveils the mechanism of a paradigmatic nickel-dependent enzyme. Angewandte Chemie. 2019;131(22):7493–7. https://doi.org/10.1002/ange.201903565

52. Berleman JE, Zemla M, Remis JP, Liu H, Davis AE, Worth AN, et al. Exopolysaccharide microchannels direct bacterial motility and organize multicellular behavior. ISME J. 2016;10(11):2620–32. https://doi.org/10.1038/ismej.2016.60 PMID: 27152937

53. Steinberg N, Kolodkin-Gal I. The matrix reloaded: probing the extracellular matrix synchronizes bacterial communities. J Bacteriol. 2015;197(13):2092–103. https://doi.org/10.1128/JB.02516-14 PMID: 25825428

54. Nadell CD, Drescher K, Wingreen NS, Bassler BL. Extracellular matrix structure governs invasion resistance in bacterial biofilms. ISME J. 2015;9(8):1700–9. https://doi.org/10.1038/ismej.2014.246 PMID: 25603396

55. Martins SG, Zilhão R, Thorsteinsdóttir S, Carlos AR. Linking oxidative stress and DNA damage to changes in the expression of extracellular matrix components. Front Genet. 2021;12:673002. https://doi.org/10.3389/fgene.2021.673002 PMID: 34394183

56. Dragoš A, Kovács ÁT. The peculiar functions of the bacterial extracellular matrix. Trends Microbiol. 2017;25(4):257–66. https://doi.org/10.1016/j.tim.2016.12.010 PMID: 28089324

57. Ivanova LA, Egorov VV, Zabrodskaya YA, Shaldzhyan AA, Baranchikov AY, Tsvigun NV, et al. Matrix is everywhere: extracellular DNA is a link between biofilm and mineralization in Bacillus cereus planktonic lifestyle. NPJ Biofilms Microbiomes. 2023;9(1):9. https://doi.org/10.1038/s41522-023-00377-5 PMID: 36854956

58. Sugimoto S, Okuda K-I, Miyakawa R, Sato M, Arita-Morioka K-I, Chiba A, et al. Imaging of bacterial multicellular behaviour in biofilms in liquid by atmospheric scanning electron microscopy. Sci Rep. 2016;6:25889. https://doi.org/10.1038/srep25889 PMID: 27180609

59. Shapiro JA. Thinking about bacterial populations as multicellular organisms. Annu Rev Microbiol. 1998;52:81–104. https://doi.org/10.1146/annurev.micro.52.1.81

60. Aguilar C, Eichwald C, Eberl L. Multicellularity in bacteria: from division of labor to biofilm formation. In: Advances in marine genomics. Springer Netherlands; 2015. 79–95. https://doi.org/10.1007/978-94-017-9642-2_4

61. Claessen D, Rozen DE, Kuipers OP, Søgaard-Andersen L, van Wezel GP. Bacterial solutions to multicellularity: a tale of biofilms, filaments and fruiting bodies. Nat Rev Microbiol. 2014;12(2):115–24. https://doi.org/10.1038/nrmicro3178 PMID: 24384602

62. Chavhan Y, Dey S, Lind PA. Bacteria evolve macroscopic multicellularity by the genetic assimilation of phenotypically plastic cell clustering. Nat Commun. 2023;14(1):3555. https://doi.org/10.1038/s41467-023-39320-9 PMID: 37322016